

# Unusual, hierarchically structured composite of sugarcane pulp bagasse biochar loaded with Cu/Ni bimetallic nanoparticles

Mengqi Tang<sup>1</sup>, Youssef Snoussi<sup>1#</sup>, Arvind K. Bhakta<sup>1#</sup>, Mohamed El Garah<sup>2,3#</sup>,  
Ahmed M. Khalil<sup>4</sup>, Souad Ammar<sup>1</sup>, Mohamed M. Chehimi<sup>1,\*</sup>

1 Université Paris Cité, CNRS, ITODYS (UMR 7086), Paris 75013, France

2 LASMIS, Antenne de Nogent – 52, Pôle Technologique de Sud – Champagne, 52800  
Nogent, France

3 Nogent International Center for CVD Innovation (NICCI), LRC CEA-LASMIS, Pôle  
Technologique de Sud Champagne, 52800 Nogent, France

4 Photochemistry Department, National Research Centre, Dokki, Giza 12622, Egypt

**\*Corresponding author:** Mohamed M. Chehimi, Université Paris Cité & CNRS,  
[mohamed.chehimi@cnrs.fr](mailto:mohamed.chehimi@cnrs.fr) ; cc: [mmchehimi@yahoo.fr](mailto:mmchehimi@yahoo.fr)

<sup>#</sup>These authors have contributed to this work equally.

## Graphical Abstract



## Abstract

Valorization of agro-wastes into high performance functional materials is a topic that is receiving growing interest. Agro-wastes could be converted into biochar by slow pyrolysis and could be even given high added value by in situ deposition of nanoparticles. Herein, we investigate for the first time the impregnation of copper and nickel nitrates on sugarcane pulp bagasse powder and its slow pyrolysis at 500 °C. The process permitted to obtain unusual hierarchically structured porous biochar material with 40 nm-sized immobilized bimetallic copper-nickel alloy nanoparticles. The materials were characterized by XRD, XPS, Raman spectroscopy, TGA and SEM. As the pure biochar does not exhibit any highly porous structure, it is suggested that copper and nickel salts, or the metallic nanoparticles, are responsible for the fishing net-like structure obtained for the underlying biochar. The alloyed metal nanoparticles are extremely well dispersed over the biochar, with narrow size distribution (40±3 nm).

This work clearly demonstrates that sugarcane pulp bagasse has a particular behavior and could provide highly porous biochar, in one step, for catalytic and other applications where high porosity and surface area are required. More importantly, such a porosity does not require any harsh acidic or basic treatment, and only the catalyst precursors are required.

### Keywords:

*Saccharum officinarum*, Sugarcane pulp, biochar, bimetallic alloy, porous materials, nanoparticles, dispersion.

## 1. Introduction

Sugarcane pulp bagasse (SCPB) constitutes the main fibrous waste product of the sugar production process after conventional grinding and juicing of sugarcane. Sugarcane grows rapidly and has high production worldwide, large amount of SCPB as a by-product is discarded after processing[1]. If bagasse is reused as a renewable raw material, it can be called one of the alternative biomass resources [2]. There are several functional groups present in sugarcane pulp bagasse, including hydroxylaliphatic, carboxyl, carbon and oxygen functional group[3] [4], which contribute to wastewater treatment [5]. However, the adsorption capacity in the environment for SCPB biomass is limited [6]. It follows that conversion of the initial biomass into biochar via slow pyrolysis is an appealing strategy to fabricate porous adsorbents for water treatment [7]. Moreover, combining biochar with immobilized catalysts is an emerging topic of great interest for efficient removal of pollutants [7, 8].

The literature shows that bimetallic catalysts are a reasonable choice, which is a combination of high activity metal and high selectivity metal, and the synergistic effect between

the two metals may improve the performance of bimetallic catalysts[9]. The two kinds of metal particles are evenly dispersed and supported on the surface of the carbonaceous material with high specific surface area, thereby supported bimetallic catalysts have higher catalytic activity through the pyrolysis process[10, 11]. Recently, we decided to tackle the preparation of bimetallic copper-nickel/biochar catalyst by direct pyrolysis of copper and nickel nitrate-impregnated olive stone powder [12, 13]. Transition metal Ni is chosen due to high activation ability of C–H and C–C bonds[14] whereas Cu is a less active transition but due to highly selective common metals[15]. The copper-nickel/ biochar served for the degradation of methyl orange and nickel imparted magnetic properties to the biochar [12, 13]. It is worth to note that bimetallic copper/nickel nanocatalysts serve for catalysing the conversion of CO<sub>2</sub> into dimethyl carbonate [16], reduction of para-nitrophenol [17] electrooxidation and nonenzymatic sensing of glucose [18], electroreduction of nitrates [19], and removal of dyes from water [20]. Copper precursors are low cost while nickel compounds are reasonably priced which make the preparation of CuNi bimetallic nanocatalyst cost effective. Moreover, it was found that catalytic activity of CuNi is superior to those of the individual monometallic nanocatalysts, on the one hand, and improved when the bimetallic nanocatalyst is dispersed on a support [17].

Despite the rich literature on CuNi bimetallic nanocatalyst, loading CuNi bimetallic nanocatalysts in- and on the surface of biochar remains sparse [21]. Our ongoing research work consisted in the direct slow pyrolysis of olive pit powder by copper and nickel nitrate mixtures under various conditions [12, 13], instead of the two-step method consisting in biochar making followed by impregnation of copper and nickel salts and their in situ reduction into bimetallic nanocatalyst, in the furnace under H<sub>2</sub> flow [21].

The aim of this work was to prepare the copper/nickel bimetallic nanoparticles-loaded sugarcane pulp bagasse biochar via slow pyrolysis at 500 °C, and to investigate the influence of agricultural waste powder was impregnated with copper and nickel nitrate prior to pyrolysis on the crystallinity, surface chemical composition, morphology, and thermal stability in air atmosphere of the biochar by X-ray diffraction (XRD), X-Ray photoelectron spectroscopy (XPS), Raman spectroscopy, scanning electron microscopy (SEM), thermogravimetric analyses (TGA) characterization. To the very best of our knowledge this is the first report on CuNi nanocatalyst loaded on sugarcane pulp bagasse by slow pyrolysis. One key feature is that the pyrolysis of the pulp bagasse impregnated with copper and nickel nitrates led to unusual porous biochar structure

loaded with bimetallic nanoparticles, without any harsh acidic or basic pretreatment of the biomass. This is what has motivated us most to report these preliminary results.

## 2. Materials and methods

### 2.1. Biomass and Chemicals

The used sugarcane bagasse was cultivated and provided from Egypt (*Saccharum officinarum*). Sugarcane pulp bagasse (SCPB) agricultural was finely ground prior to use. Metal nitrate salts  $\text{Cu}(\text{NO}_3)_2 \cdot 3\text{H}_2\text{O}$  and  $\text{Ni}(\text{NO}_3)_2 \cdot 6\text{H}_2\text{O}$  were purchased from Aldrich and used as received. We used distilled water to dissolve metal nitrates before pyrolysis.

### 2.2. Synthesis of biochar loaded with Cu/Ni bimetallic nanoparticles

SCPB particles were impregnated with an aqueous copper and nickel solution (0.5/0.5 mmol initial molar ratio of  $\text{Cu}(\text{NO}_3)_2 \cdot 3\text{H}_2\text{O}/\text{Ni}(\text{NO}_3)_2 \cdot 6\text{H}_2\text{O}$  each per 1 g SCPB using a minimal amount of deionized water) (see Figure 1). Stir the powder on a glass lens with a spatula and dry at 40 degrees until the powder did not change in weight. Subsequently, the mixture containing CuNi-impregnated particles was transferred into a tube furnace and prepared at 500 °C by pyrolysis at  $\text{N}_2$  atmosphere for 1h with a heating rate of 20 °C  $\text{min}^{-1}$ . The same agrowaste SCPB without any metallic nitrate was pyrolyzed at same condition.

**Table 1.** Preparation of Pure Biochar and Metallic Nanoparticle-Coated Biochar including pyrolysis conditions.

Materials	P-SCB Mass(g)	$\text{Cu}(\text{NO}_3)_2 \cdot 3\text{H}_2\text{O}$ Mass (g)/mmol	$\text{Ni}(\text{NO}_3)_2 \cdot 6\text{H}_2\text{O}$ Mass (g)/mmol	Distilled water (mL)	Before Pyrolyzed SCB+Metal Ion Mixture(g)	Biochar Mass (g) /Yield (%)	Experimental condition
SCPBB@CuNi	0.996	120.8/0.5	145.4/0.5	20	1.226	0.352/28.71	Temperature: 500 °C Heating rate: 20 °C · min Residence time: 1 h Gas: $\text{N}_2$ atmosphere $\text{N}_2$ flow rate: 2L · $\text{min}^{-1}$
SCPBB	2.143	/	/	/	/	0.504/23.51	

### ***2.3. Materials Characterization***

The XRD patterns of carbon powder samples were performed in the range  $20^{\circ} \leq 2\theta \leq 80^{\circ}$  using a D8 Advance Bruker diffractometer (Cu K $\alpha$  radiation) with X-ray generator voltage of 40 kV and the current of 40 mA., and step size of  $0.33^{\circ}$  using scan speed  $1.11^{\circ} \cdot \text{s}^{-1}$ . The applying of a technique through the use of the Highscore and Origin software line shape to the peaks.

XPS spectra of biochars were recorded using a K Alpha+ apparatus (Thermo, East Grinstead, UK). The machine is fitted with a mono Al K $\alpha$  (source energy = 1486.6 eV), and a flood gun for charge compensation build up. The pass energy was set to 200 eV to record the survey spectra and 80 eV for the acquisition of the narrow regions. Avantage software version 5.9902 was used for data acquisition and processing.

Raman spectra analysis was conducted by a Horiba HR 800 instrument to determine the carbon signature at a wavelength of the He–Ne laser beam set to 633 nm. The spectrum recorded in the  $800\text{--}2700 \text{ cm}^{-1}$  energy region for the biochar without metal nanoparticles.

We have employed a Hitachi SU 8030 Scanning Electron Microscope (SEM) Field Emission Gun (FEG) SEM for the observation of the samples morphology. No charge compensation was used, and the source-sample distance was set at 4.2 mm. ImageJ software was used for SEM images processing.

TGA conducted were conducted using a Setaram machine Setsys Evolution model to measure the mass loss kinetics of biochar (with or without metallic nanoparticles). The experiments were performed over a temperature range of ambient from  $30^{\circ}\text{C}$  to  $800^{\circ}\text{C}$  using a constant heating rate of  $10^{\circ}\text{C}/\text{min}$  under air atmosphere.

### 3. Results and Discussion

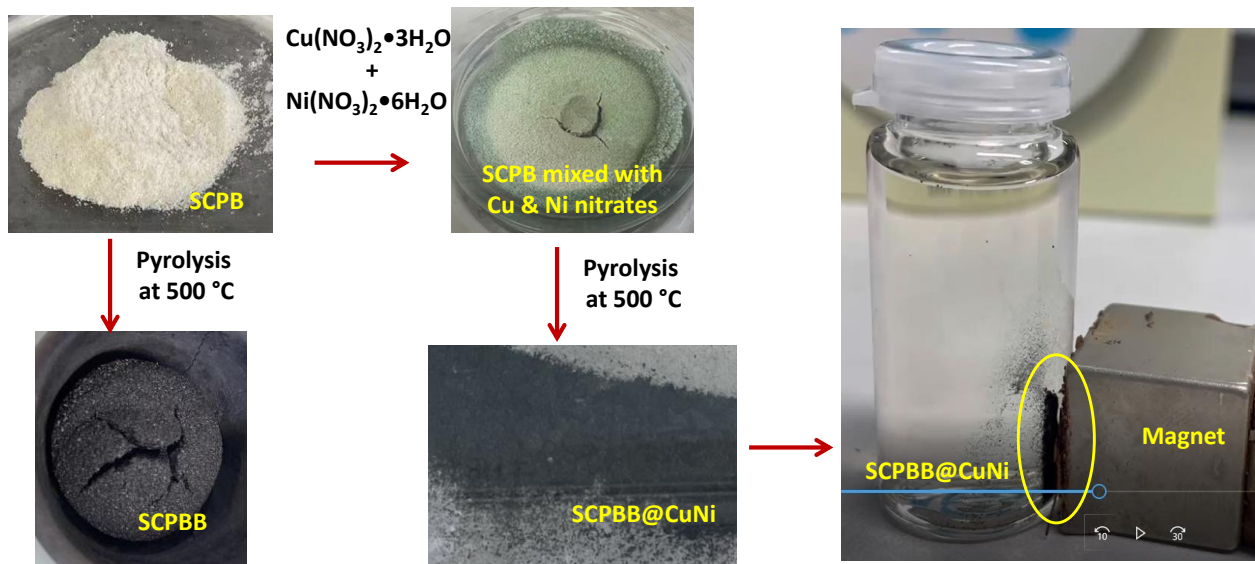


**Figure 1.** General pathway for making bare biochar and magnetic copper nickel nanoparticle-loaded biochar by slow pyrolysis. Right hand side picture: NB: the SCPBB@CuNi biochar powder attracted by a magnet is circled in the right hand side picture.

We have adopted the method devised by Khalil *et al.* [12], however with some modifications concerning the initial masses and pyrolysis conditions. The main difference is the use of sugarcane pulp bagasse, which is rather not explored in the literature compared to the total sugarcane bagasse. The final SCPBB@CuNi is easily attracted by a magnet, despite the two-fold lower content of CuNi.

The XRD analysis were conducted on bare SCPBB and copper nickel nitrate impregnation of biochar. The diffractogram correspond to SCBPP@CuNi and reference biochar in Figure 2. The XRD pattern displays two corresponding peaks at at 51.5°, 59.8° and assigned to structures of copper nickel metals (111), (002) crystallographic planes, respectively (ICSD n 98-062-8543). This indicates that SCBPP@CuNi showed the presence of a crystalline structure, copper nickel as alloy was produced with the pyrolysis of copper nickel nitrate-impregnated biomass.

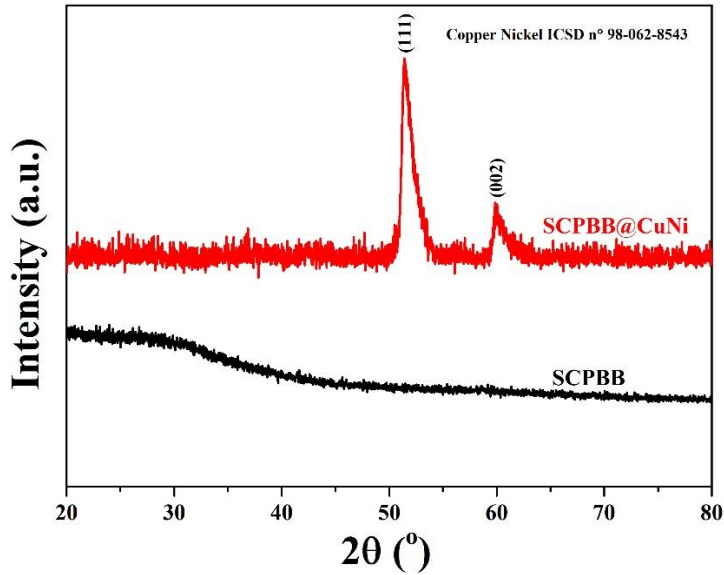


**Figure 2.** XRD patterns of SCPBB and SCPBB@CuNi composite.

Figure 3 displays the XPS survey spectra of the biochar (Figure 3a) and the SCPBB@CuNi (Figure 3b). Cu2p and Ni2p are shown in inset and testify for the presence of these elements in the metallic states (Ni2p<sub>3/2</sub> at ~852.1 eV; sharp Cu2p<sub>3/2</sub> peak centred at 932.1 eV). Surface oxidation is also noted for nickel as evidenced by the oxide peak (855.3 eV) and its satellite (860.7 eV). A shake up satellite too is noted for copper (843.9 eV) and is characteristic of Cu(II) oxidation state [22]. The Cu/Ni atomic ratio is ~2, two fold higher than the expected one, indicating possible preferential occurrence of copper at the surface of the NPs.

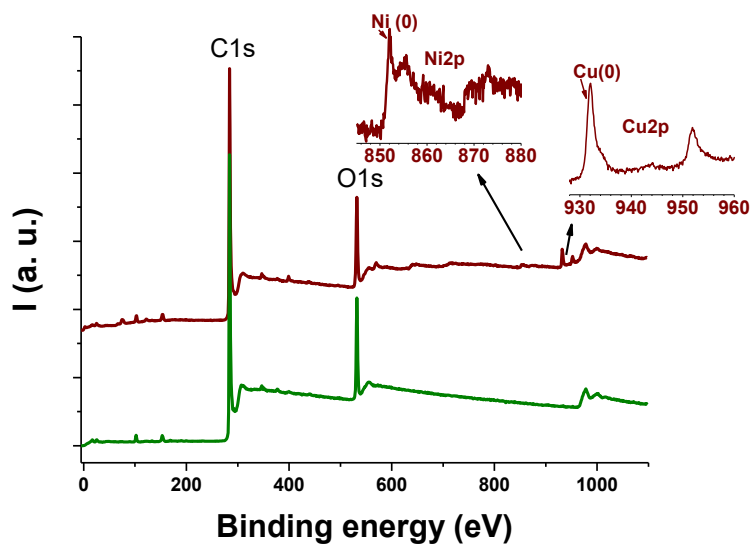


**Figure 3.** XPS spectra of pure biochar (a) and SCPBB@CuNi (b).

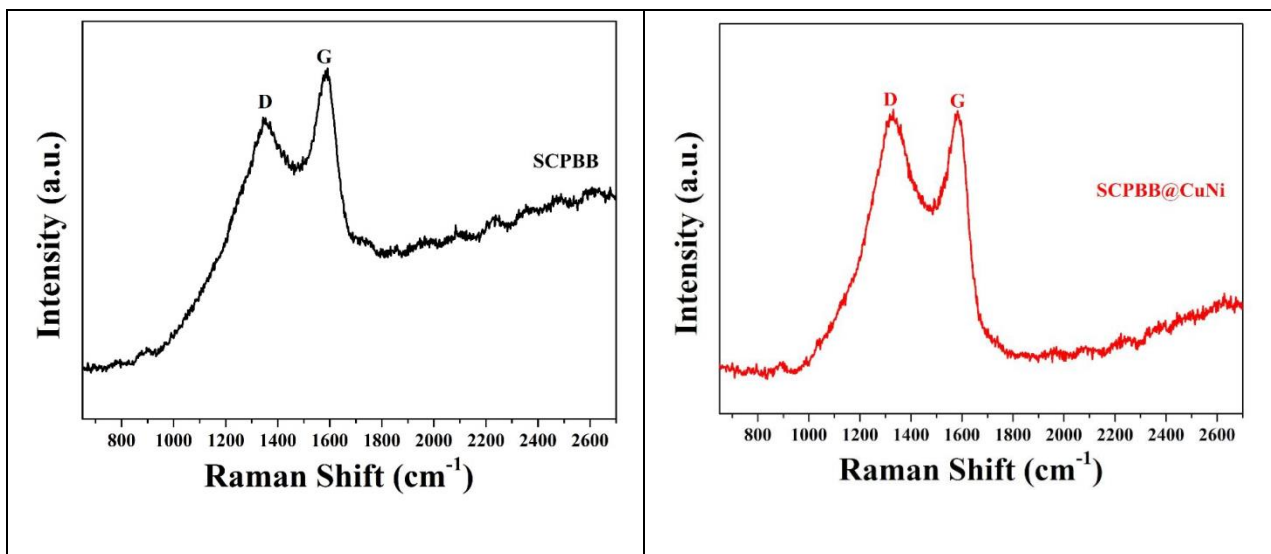


**Figure 4.** Raman spectra of bare SCPBB biochar and SCPBB@CuNi obtained at 500 °C.

In order to have further insights into the structural transformations of bare SCPBB and to infer the presence of graphitic characteristics [23, 24], biochar was investigated by Raman spectroscopy with 633 nm laser to assess the degree of carbonation of carbonaceous materials [25]. The Raman spectrum of biochar from 650 to 2700  $\text{cm}^{-1}$  is shown in Fig. 4. The two

prominent bands at  $1346$  and  $1588\text{ cm}^{-1}$  are assigned to D-band (represents disordered) and G-band (represents graphitic), respectively [26, 27]. Some researchers have proposed that bagasse biochars contain multi-layer-like or graphene oxide-like organizational structures [24, 25, 28]. The  $I_D/I_G$  ratio = 0.91 for pure biochar, quasi matching 0.97 for SCPBB@CuNi. The sharp G bands indicate relatively high degree of graphitization of the biochar [29].

The thermogravimetric (TG) curves for the bare biochar and SCPBB@CuNi are shown in Figure 5. Thermal analysis was conducted in air to monitor the thermal stability and determining the mass loading. These curves shows the residual weight % of CuNi-decorated biochar is higher than that of SCPBB at a high temperature, the weight loss of SCPBB about 90% at  $800\text{ }^\circ\text{C}$ . The addition of copper and nickel to biochar resulted in significantly higher residual weight %, although biochar decomposed. Copper and nickel from the bimetallic NPs convert to metallic oxides, hence SCPBB@CuNi yields slightly higher weight %.

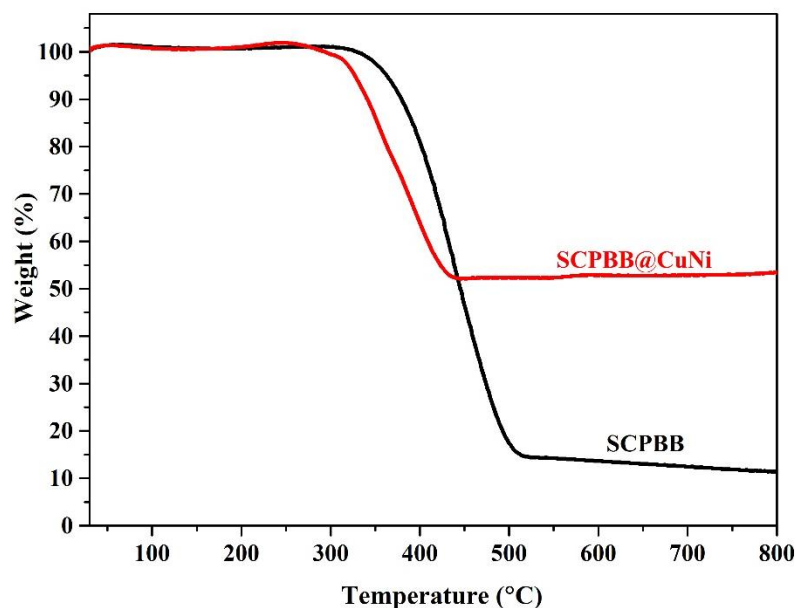


**Figure 5.** TG curves of SCPBB and SCPBB@CuNi. Analysis in air; heating rate =  $10\text{ }^\circ\text{C min}^{-1}$ .

Representative SEM micrographs of two biochars with or without CuNi NPs are shown in Figure 6a-g. The biochar SCPBB@CuNi (Figure 6a-d) is observed at various magnifications; it forms the ordered arrangement with uniform pores, similar to fishing net. The pores are

elongated, almost like slits with length in the 3 to 12  $\mu\text{m}$  range and  $\sim 1 \mu\text{m}$  slit width (Figure 6a). The pores are of smaller size, which is ascribed to dehydration of the cell structure. Nanoparticles start to be visible in Figure 6b, but are very well distinguished in Figure 6c; the NPs are densely and homogeneously dispersed over the surface avoiding any aggregates. This conforms with our previous findings [12] on CuNi bimetallic NPs loaded on olive stone powder biochar. The protocol is therefore very well reproducible and yields similar results on a different biomass (herein sugarcane pulp bagasse). The presence of porous structure in the SCPBB@CuNi sample ensures they can increase the properties during the adsorption or catalytic processes. From 6d, one could estimate the average CuNi nanoparticle size to  $40 \pm 3 \text{ nm}$ . The SCPB-derived biochar exhibits plainer surface compared to SCPBB@CuNi (Figures 6e-g) with only fewer micrometer-sized pores. It follows that the activation of the biomass with copper and nickel nitrates favours the formation of slits, and therefore the highly porous structure without any use of harsh acidic or basic media. Indeed, the slits shown in Figures 6a-c seems to originate from the pores exhibited by the SCPBB biochar (Figures 6f,g).

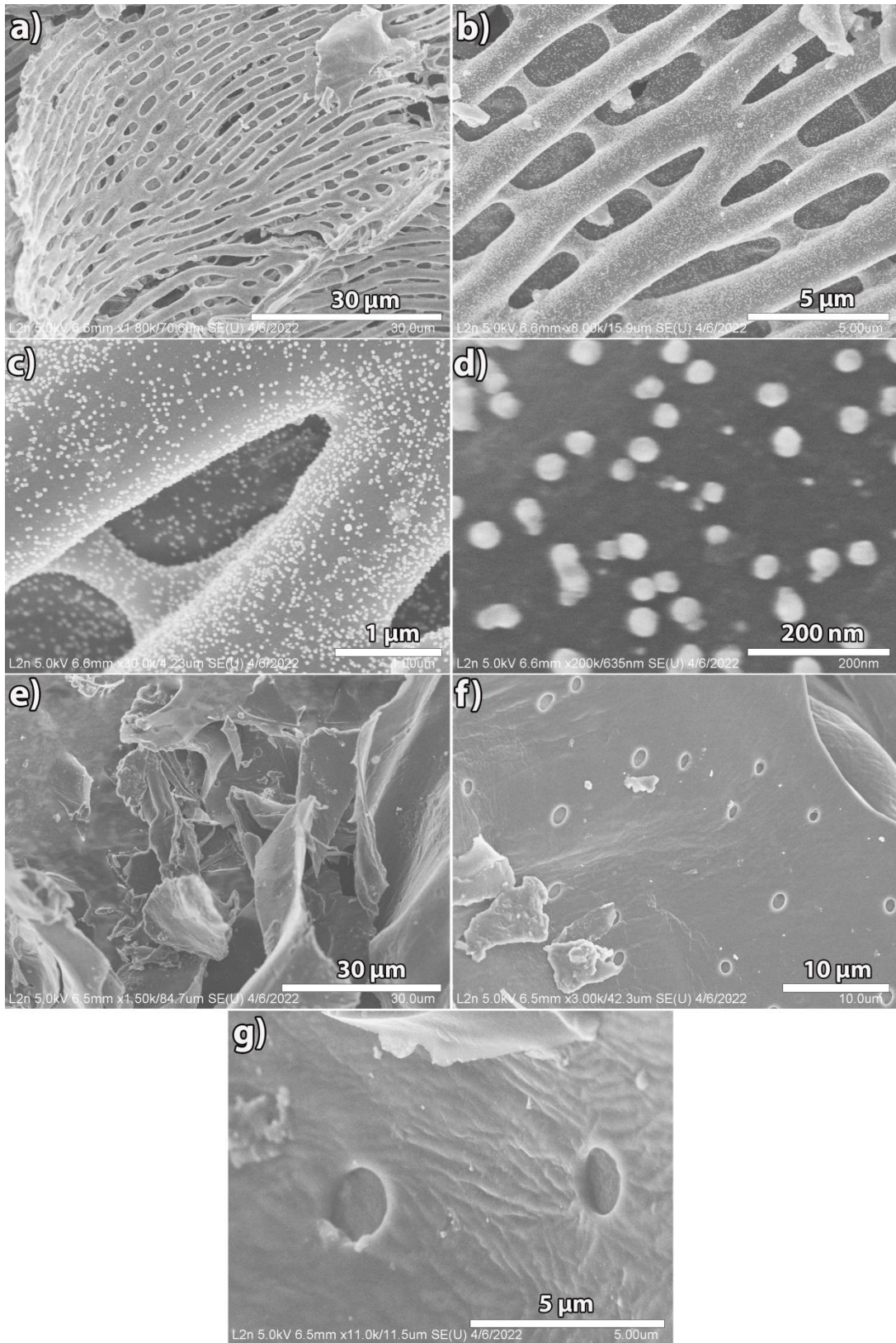


**Figure 6.** SEM images of SCPBB@CuNi (a-d) and SCPBB (e-g) at various magnifications.

#### **4. Conclusion**

To sum up, bimetallic copper-nickel alloy nanoparticles were prepared over highly porous sugarcane pulp bagasse biochar (SCPBB@CuNi), in one step by slow pyrolysis at 500 °C for 1h. The material exhibits unusual hierarchical micro/nano structure. Biochar arranged in an usual network resembling to fishing net with decorated ~40 nm-sized bimetallic nanoparticles is magnetic due to the presence of nickel. Unlike olive stone biochar, impregnation of the initial sugarcane pulp bagasse with copper and nickel nitrates results in an un-expected highly porous structure induced by the metal salts. This study demonstrates that impregnation of biomass with copper and nickel nitrates yield biochar@CuNi with evenly dispersed alloyed CuNi nanoparticles.

We are exploring the process with other biomasses in order to determine whether and why a given initial biomass is prone to the highly porous structure demonstrated in this work, or if this is mainly due to metallic salts, or if there is any synergetic biomass/metal salt effects.

#### **Acknowledgements.**

P. Decorse, Mrs S. Lau-Truong and Alexandre Chevillot-Biraud (experimental officers at ITODYS lab) are acknowledged for their assistance with XPS, Raman and TGA measurements, respectively.

#### **Funding**

We thank the China Scholarship Council for the provision of PhD scholarship to Mengqi Tang (No 202008310221). Wallonie Bruxelles International (WBI) is acknowledged for the provision of a grant “Bourse WBI Excellence World” (No Imputation 101386, Article Budgétaire 33.01.00.07). A.M.K. and M.M.C. would like to thank the French government for funding A.M.K.’s contribution through a fellowship granted by the French Embassy in Egypt (Institut Francais d’Egypte).

#### **Conflict of Interest**

The authors declare no conflict of interest

## References

1. Aruna, et al., *A review on modified sugarcane bagasse biosorbent for removal of dyes*. Chemosphere, 2021. **268**: p. 129309.
2. Bordonal, R.D., et al., *Sustainability of sugarcane production in Brazil. A review*. Agronomy for Sustainable Development, 2018. **38**(2).
3. Yang, Z.H., et al., *Cr(III) adsorption by sugarcane pulp residue and biochar*. Journal Of Central South University, 2013. **20**(5): p. 1319-1325.
4. Yang, Z.H., et al., *Removal of Cr(III) and Cr(VI) from aqueous solution by adsorption on sugarcane pulp residue*. Journal Of Central South University Of Technology, 2009. **16**(1): p. 101-107.
5. Gupta, V.K., et al., *Removal of cadmium and nickel from wastewater using bagasse fly ash - a sugar industry waste*. Water Research, 2003. **37**(16): p. 4038-4044.
6. Ngah, W.S.W. and M. Hanafiah, *Removal of heavy metal ions from wastewater by chemically modified plant wastes as adsorbents: A review*. Bioresource Technology, 2008. **99**(10): p. 3935-3948.
7. Sutar, S., P. Patil, and J. Jadhav, *Recent advances in biochar technology for textile dyes wastewater remediation: A review*. Environmental Research, 2022: p. 112841.
8. Lopes, R.P. and D. Astruc, *Biochar as a support for nanocatalysts and other reagents: Recent advances and applications*. Coordination Chemistry Reviews, 2021. **426**: p. 213585.
9. Pang, J.F., et al., *Catalytic conversion of cellulose to hexitols with mesoporous carbon supported Ni-based bimetallic catalysts*. Green Chemistry, 2012. **14**(3): p. 614-617.
10. Liu, R.H., et al., *Multi-scale complexities of solid acid catalysts in the catalytic fast pyrolysis of biomass for bio-oil production - A review*. Progress In Energy And Combustion Science, 2020. **80**.
11. Yao, D. and C.H. Wang, *Pyrolysis and in-line catalytic decomposition of polypropylene to carbon nanomaterials and hydrogen over Fe- and Ni-based catalysts*. Applied Energy, 2020. **265**.
12. Khalil, A.M., et al., *Copper/nickel-decorated olive pit biochar: One pot solid state synthesis for environmental remediation*. Applied Sciences, 2021. **11**(18).
13. Omiri, J., et al., *Citric-Acid-Assisted Preparation of Biochar Loaded with Copper/Nickel Bimetallic Nanoparticles for Dye Degradation*. Colloids and Interfaces, 2022. **6**(2).
14. Liao, M.Z., et al. *Efficient hydrogen production from partial oxidation of propane over SiC doped Ni/Al<sub>2</sub>O<sub>3</sub> catalyst*. in *10th International Conference on Applied Energy (ICAE)*. 2018. Hong Kong, HONG KONG.
15. Hu, L.Y., et al., *Direct hydroxylation of benzene to phenol on Cu-V bimetal modified HMS catalysts*. Catalysis Communications, 2014. **43**: p. 179-183.
16. Chen, Y., et al., *Porous diatomite-immobilized Cu-Ni bimetallic nanocatalysts for direct synthesis of dimethyl carbonate*. J. Nanomaterials, 2012. **2012**: p. Article 8.
17. Deka, P., et al., *Cu-Based Nanoparticles as Emerging Environmental Catalysts*. The Chemical Record, 2019. **19**(2-3): p. 462-473.
18. Zhang, C., et al., *In-situ facile preparation of highly efficient copper/nickel bimetallic nanocatalyst on chemically grafted carbon nanotubes for nonenzymatic sensing of glucose*. Journal of Colloid and Interface Science, 2019. **557**: p. 825-836.
19. Mirzaei, P., *Préparation de matériaux d'électrode pour l'élimination et la valorisation de polluants azotés*. 2018, Paris Est.
20. Younas, U., et al., *Antioxidant and Organic Dye Removal Potential of Cu-Ni Bimetallic Nanoparticles Synthesized Using Gazania rigens Extract*. Water, 2021. **13**(19).

21. Zhu, C., et al., *Selective Hydrodeoxygenation of 5-Hydroxymethylfurfural to 2,5-Dimethylfuran over Alloyed Cu–Ni Encapsulated in Biochar Catalysts*. ACS Sustainable Chemistry & Engineering, 2019. **7**(24): p. 19556-19569.
22. Biesinger, M.C., *Advanced analysis of copper X-ray photoelectron spectra*. Surface and Interface Analysis, 2017. **49**(13): p. 1325-1334.
23. Dong, Q., et al., *Engineering porous biochar for capacitive fluorine removal*. Separation And Purification Technology, 2021. **257**.
24. da Silva Veiga, P.A., et al., *Production of high-performance biochar using a simple and low-cost method: Optimization of pyrolysis parameters and evaluation for water treatment*. Journal Of Analytical And Applied Pyrolysis, 2020. **148**.
25. da Silva Veiga, P.A., et al., *Upgrading from batch to continuous flow process for the pyrolysis of sugarcane bagasse: Structural characterization of the biochars produced*. Journal Of Environmental Management, 2021. **285**.
26. Debalina, B., R.B. Reddy, and R. Vinu, *Production of carbon nanostructures in biochar, bio-oil and gases from bagasse via microwave assisted pyrolysis using Fe and Co as susceptors*. Journal Of Analytical And Applied Pyrolysis, 2017. **124**: p. 310-318.
27. Ahmad, E., et al., *Integrated thermo-catalytic reforming of residual sugarcane bagasse in a laboratory scale reactor*. Fuel Processing Technology, 2018. **171**: p. 277-286.
28. Sen Gupta, S., et al., *Graphene from Sugar and its Application in Water Purification*. Acs Applied Materials & Interfaces, 2012. **4**(8): p. 4156-4163.
29. Chia, C.H., et al., *Imaging of mineral-enriched biochar by FTIR, Raman and SEM-EDX*. Vibrational Spectroscopy, 2012. **62**: p. 248-257.